Conductance distribution in doped and defected graphene nanoribbons

Antonino La Magna
CNR–IMM, Z.I. VIII Strada 5, 95121 Catania, Italy

Ioannis Deretzis
Scuola Superiore, Università di Catania, I-95123 Catania, Italy and CNR–IMM, Z.I. VIII Strada 5, 95121 Catania, Italy

Giuseppe Forte
Dipartimento di Scienze Chimiche, Facoltà di Farmacia, Università di Catania, Viale A. Doria 6, I-95126 Catania, Italy

Renato Pucci
Dipartimento di Fisica e Astronomia, Università di Catania and CNISM, UdR di Catania, Via S. Sofia 64, I-95123 Catania, Italy
(Received 29 August 2009; revised manuscript received 7 October 2009; published 17 November 2009)

Electronic transport at the μm length scale is theoretically investigated for *N*-doped and vacancy damaged graphene nanoribbons. In these systems, localization due to scattering is strongly energy dependent, and this fact leads to the appearance of conductance quasigaps in the spectral region of the resonance states. Conductance fluctuations are very large in the quasigap regions and increase linearly with the system size. The single parameters scaling hypothesis is not verified for energies in a zone including the charge neutrality point while it is valid for energies away from this zone.

DOI: 10.1103/PhysRevB.80.195413 PACS number(s): 72.10.Fk, 72.15.Rn, 73.23.−b, 73.63.−b

I. INTRODUCTION

Graphene can be considered a material with potentially exceptional electronic properties like high room temperature mobility and ballistic conduction for submicroscale lengths, which, in view of the post-Si electronic applications, are hindered by the presence of a minimum of the conductivity. Electron confinement, realized by means of nanostructures[1] or strain engineering[2] (i.e., through geometric confinement), could overcome these difficulties. In this sense, the most promising systems for graphene-based nanoelectronics are the graphene nanoribbons (GNRs), which have been already synthesized by means of different pattering techniques.[3,4] In these cases, the control of the electronic properties is inherently related to the accurate manipulation of the nanostructure edges. However, also the chemical modification of the system bulk zone, e.g., using substitutional impurities, has been proposed to overcome the minimum of conductivity problem.[5,6] This prospect also meets the more basic studies of the disorder effect on graphene-based systems,[7] which is a central problem in graphene due to production faults, surface exposition and the influence of the substrate (strongly bounded to the GNRs in the case of flakes grown on SiC).[8]

It is highly likely that the undergoing development of graphene nanostructures will soon make possible a systematic experimental study of quantum transport fundamentals in low-dimensional disordered systems, which nowadays have been mainly the subject of theoretical investigations. In a recent work, the validity of the single parameter scaling (SPS) hypothesis, i.e., the universal dependence of the conductance distribution function on the localization length ξ, has been critically addressed in strongly disordered GNRs in the framework of the Anderson model.[9] However, these findings have to be confirmed in more realistic descriptions of graphene-based conductors, since the Anderson model is a rather idealized realization of the real disorder (or the real chemical modification) that could be approximately valid in the case of a huge density of local scattering centers.[10]

In this work, we have extensively investigated, by means of *ab initio* calibrated models and nonequilibrium Green's function (NEFG) techniques, the effects of the inclusion of controlled densities of local scattering centers, i.e., vacancies (*V*'s) and *N* impurities, in the conductance distribution function of large (up to ~ 1 μm) Armchair GNRs (AGNRs). Simulations have been performed for large replicas of equivalent systems and results represent statistical averages over conductance-related properties. The computational outcomes reveal that the validity of the single parameters scaling hypothesis is not universal, but rather depends on the vicinity of the energy position with respect to the charge neutrality level of the studied systems. In addition, characteristics of disorder induced (pseudo)gap issues are also addressed.

The article is organized in the following way: Sec. II gives a brief overview of the computational methodology, Sec. III presents statistical analyses of the conductance in doped and defected GNRs, and Sec. IV presents density of states criteria for the evaluation of the SPS hypothesis, while in Sec. V we discuss our results.

II. METHODOLOGY AND CALIBRATION

AGNRs are classified using the convention of Ref. 1, i.e., with the integers N_a indicating respectively the number of dimer lines across the ribbon width. The system length *L* is also indicated by an integer which is the number of atoms belonging to the dimer lines ($L \in [500, 4000]$ in this work, while the maximum length considered corresponds to about 0.84 μm). Consistently with graphene's electronic bandstructure, we assume that only p_z orbitals contribute to the transport mechanism along the GNR. For efficiency's sake,

we neglect the contributions of the hopping term between p_z orbitals in the second neighbor shell and above (nearest-neighbor tight-binding approximation). *Ab initio* calculations have been used in order to calibrate the Hamiltonian matrix elements in correspondence with local or extended alterations of the periodicity: i.e., impurities,[11] defects,[10,12] and ribbon edges.[1]

In the case of Nitrogen impurities and similarly to the case of Boron discussed in Ref. 6, the calibration of the Hamiltonian matrix elements corresponding to atomic positions near the impurity implies a significant modification of the diagonal elements only. The extension (about 1 nm) of the resulting scattering potential is larger than the 10th neighbor shell distance with respect to the impurity site. Using a different AB INITIO code[13] with an equivalent basis set, we have verified that the properties of the scattering potential are similar to that reported in Ref. 11, considering the case of a graphene sheet.

On the other hand, the simplest and mostly used method[7,14,15] to include a vacancy in a given GNR site i is just by removing the site from the model, switching to zero the related hopping t_{ij} terms or, equivalently switching to infinite the related on site term ε_i. The corresponding mode (also called *zero energy mode*) has a series of characteristics due to the graphene bipartite lattice which have been exhaustively studied in Ref. 7. A particular consequence of the symmetry of the zero mode should be an on/off switching of the low bias conductance in contacted graphene quantum dots depending on the contact's location.[12] *Ab initio* calculations have excluded such a behavior since states around the charge neutrality points do not show zero-energy mode symmetries. Moreover, opposite to the impurity case and due to the bond reconstructions, the vacancy presence significantly alters also the off-diagonal sector of the Fock matrix projected on the p_z orbitals. As a consequence, in order to obtain a reliable and effective calibration of the V-type defect in a nearest-neighbor tight-binding Hamiltonian, the on-site and hopping terms relative to the site occupied by the defects has been tuned in order to obtain states around the charge neutrality point which reproduce the correct symmetries (and the correct conductance features including the lacking of the cited on/off switch) of the *ab initio* calculations.[12] The tuned values are $\varepsilon_i=10$ eV and $t_{ij}=1.9$ eV (to be compared to the 2.7 eV values of the perfect lattice).

H passivation of dangling bonds at the GNR edges is included in the Hamiltonian following the calibration, based on *ab initio* calculations, reported in Ref. 1, i.e., modifying the hopping integral of C–C bonds at the edge. This correction leads to the appearance of a small gap at the charge neutrality point for GNRs with $N_a=3\times n+2$, where n is an integer number. These GNRs are otherwise perfectly metallic in the approximation considered.

A two-terminal device geometry is considered throughout the article where the randomly doped or defected region corresponds to the whole active device's part. The key quantity calculated here by means of optimized numerical techniques[9] is the zero-bias/temperature conductance $g(E)=(2e^2/h)T(E)$ at energy E (which in the following will be reported in $2e^2/h$ units), where T is the transmission coefficient within the Landauer approach. The latter can be calculated using the NEGF formalism as $T=Tr[\Gamma_L G \Gamma_R G^\dagger]$, where $G=(E^+I-H-\Sigma_L-\Sigma_R)$ is the Green's function of the system, I is the identity operator, Σ_L,Σ_R are the self-energies including the effect of scattering due to the left (L) and right (R) contacts, and $\Gamma_{L,R}=i(\Sigma_{L,R}-\Sigma_{L,R}^+)$ are the contact spectral functions. Semi-infinite contacts are considered in this work with self-energies $\Sigma=\tau g_s \tau^\dagger$, where g_s is the surface Green's function of the respective lead and τ is the conductor-contact interaction.[16] Contacts are of the same width N_a as the conductor without defect or impurity inclusions.

III. STATISTICAL ANALYSIS OF THE CONDUCTANCE IN DOPED AND DEFECTED AGNRS

The conductance energy dependence of a disordered GNR due to a random inclusion of defects or impurities shows significant alteration with respect to that of an ideal system. Indeed, in correspondence to the plateaus of the ideal conductance curve, a strongly fluctuating conductance has been calculated for disordered systems, where peaks eventually reach the plateau levels, while the electron-hole symmetry of the spectrum is completely broken.[16] Of course, the spectrum significantly changes with the given disorder realization even when we fix the system's size and the density of scattering centers. In order to correlate systematically the conductance features to the disorder realization, average conductance has been calculated in a large number of statistically equivalent replicas of the same system (i.e., same size and impurity density) in the case of B-doped GNRs.[6] In the latter work, 1 eV large mobility gap in the average conductance spectrum have been estimated, and this evidence should indicate that chemically doped GNRs could solve the problem related to the conductivity minimum of graphene-based devices. However, in the practical use of multiple electronic devices in an integrated system, an equivalent behavior of the single device is required within a given tolerance window. As a consequence, the variance of the conductance could be an additionally important parameter to be calculated in these statistical analyses of disordered systems in view of nanoelectronic applications. Moreover, a complete statistical study, as we will see, could be interesting with respect to the fundamentals of theoretical and experimental research of disordered and low dimensional systems.

Average conductance and the variance of the logarithm of the zero temperature conductance

$$\sigma^2=\langle(\ln g)^2\rangle-\langle\ln g\rangle^2 \tag{1}$$

are shown in Fig. 1 as functions of the energy for a 47-AGNR doped with a 0.2% density of N atoms and for systems with increasing length L, from $L=500$ (~ 0.1 μm) to $L=4000$ (~ 0.8 μm). Natural logarithms are used in Eq. (1) and in other expressions in this work. In doped systems, significant (nonsymmetric) decreases in the average conductance with respect to the pure system can be observed in particular spectral regions (note that the charge neutrality points are aligned at $E=0$ for both doped and pure systems). In particular, in the energy region near the single impurity resonance states (i.e., for energies near the electron edge $E\sim 0.25$ eV of the first plateau of the conductance for the pure

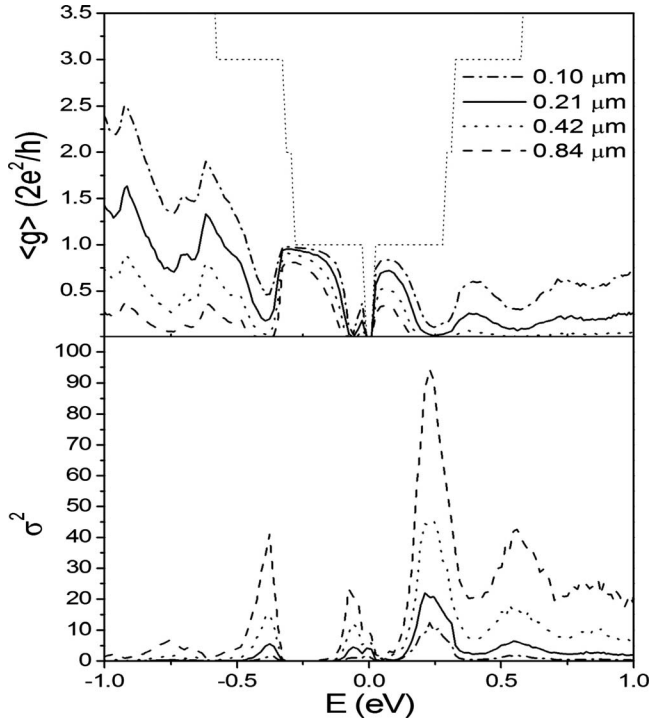

FIG. 1. Average conductance ⟨g⟩ (a) and conductance fluctuations σ^2 (b) as a function of the energy E, for an N doped N_a =47-AGNR of different lengths: L=500 (dashes and dots), 1000 (solid lines), 2000 (dots), and 4000 (dashes). The lengths in μm are also reported. Plotted values represent statistical averages over more than 500 equivalent replicas of the system. Charge neutrality points of pure and doped systems are aligned at E=0 in the figure.

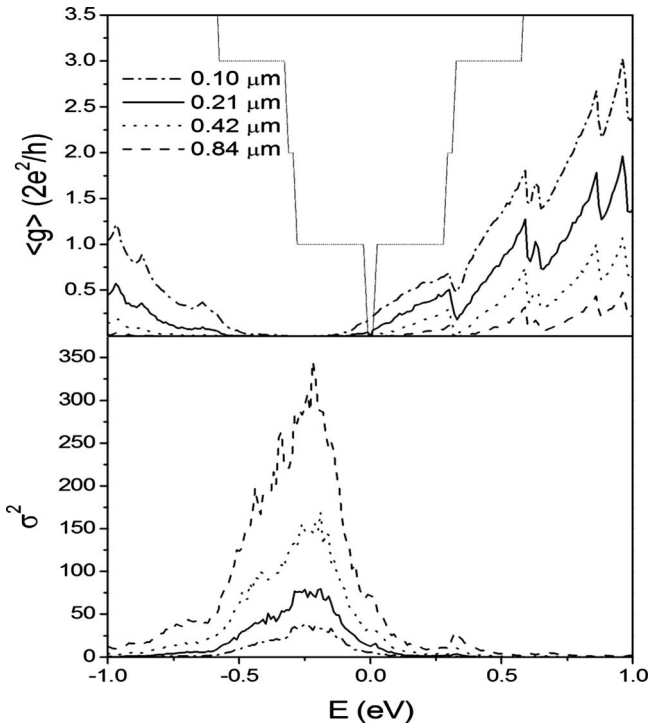

FIG. 2. Average conductance ⟨g⟩ (a) and conductance fluctuations σ^2 (b) as a function of the energy E, for a V-damaged N_a =47 AGNR of different lengths: L=500 (dashes and dots), 1000 (solid lines), 2000 (dots), and 4000 (dashes). The lengths in μm are also reported. Plotted values represent statistical averages over more of 500 equivalent replicas of the system. Charge neutrality points of pure and defected systems are aligned at E=0 in the figure.

system) a quasigap appears also for the smaller systems. This quasigap extends asymmetrically in the electron band ($E>0$) beyond this region for larger systems. Equivalent behavior has been reported in Ref. 6 for the case of B-doped GNRs apart of course the different location of the quasigap in the spectrum. Our numerical analysis has established that these systems are in the localized regime for energies within the quasigap: i.e., with a good confidence the average zero temperature resistance $r(E)=g(E)^{-1}$ depends exponentially on L, therefore,

$$\langle \ln r(E) \rangle = 2L/\xi(E) + c, \tag{2}$$

where c is a small constant that does not depend on E and $\xi(E)$ is the energy dependent localization length. In particular, in the studied systems the transition from the weak localization regime [$L<\xi/E$)] to the strong localization regime [$L>\xi(E)$] depends on: the value of the energy, the type of scattering centers (impurity or vacancy) and the density of scatter centers. As an example, the interval of the $\xi(E)$ values measured in a number of dimer lines is $\xi(E) \in [232, 2954]$ for the data shown in Fig. 1, and generally the smaller values of $\xi(E)$ are obtained for energies corresponding to the conductance dips. These dips are characterized by large values of the conductance fluctuation [compare Figs. 1(a) and 1(b)]. In particular, the variance [Eq. (1)] has a large peak in the energy region of the resonance states. In general, dips of the average conductance are related to peaks of the variance, apart for energies near the small gap at the charge neutrality point[1] where conductance fluctuations are relatively small.

A qualitatively similar behavior is shown by the V-damaged systems (see Fig. 2 $\xi(E) \in [57, 3414]$ in this case). However, here, a larger pseudogap appears in the negative energies (hole band) region also for the smaller systems due to the stronger backscattering of the defects with respect to the impurities. This pseudogap is not centered around E=0 as we should expect for an idealized V description (i.e., an infinite ε_i scattering center).[6] Indeed, as we have noted, *ab initio* calculations have evidenced that due to the bond's reconstruction, Vs in graphene-based systems have not exactly the behavior of zero energy modes but an impurity-like behavior. Again, due to the stronger backscattering in correspondence to the pseudogap the variance assumes relatively larger values in defected systems with respect of the doped ones [compare Figs. 1(b) and 2(b)].

Our statistical analysis shows a linear dependence of $\sigma(E,L)^2$ on the system length L for fixed values of the system quasi-Fermi energy E. A similar finding, expected in pure one-dimensional systems, was previously recovered in quasi-one-dimensional GNRs (Ref. 9) where the disorder was realized in the framework of the Anderson model.[17] A peculiar aspect of the GNRs conductance distribution is the failure of the SPS hypothesis when strong local fluctuations of the on-site potential are the source of backscattering.[9] SPS

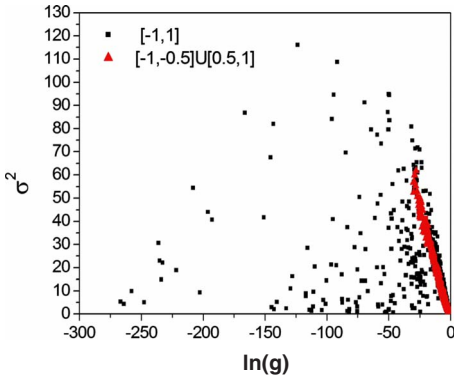

FIG. 3. (Color online) Conductance fluctuations σ^2 as a function of the average of the conductance natural logarithm $\langle \ln(g) \rangle$ for different N-doped $N_a=45$ AGNRs. Each point represents a statistical average over more of 500 equivalent replicas of the system. The systems differ for: scatter center density (0.2%, 0.4% cases), Fermi energy E, which belongs to the interval $[-1,1]$ and length $L=500,1000,1500,2000,4000$. Red triangles evidence points for energies E in the intervals $[-1,-0.5]$ and $[0.5,1]$.

states that the conductance distribution is a universal function of ξ and, as a consequence, also σ^2 depends only on the localization length. In Figs. 3–5 σ^2 is shown (black squares) as a function of $\langle \ln g(E) \rangle$ [and due to the validity of Eq. (2) implicitly as a function of $2L/\xi$]: for an N-doped 45-AGNR (Fig. 3, $\xi(E) \in [274,2754]$), an N-doped 47-AGNR (Fig. 4, $\xi(E) \in [206,5355]$), and a defected 47-AGNR (Fig. 5, $\xi(E) \in [44,3414]$). Each point represents a statistical analysis on more than 500 replicas of the systems. Conductance distribution was evaluated in systems of different lengths in the $L=500-4000$ ($\sim 0.1-\sim 0.84$ μm) range and different impurity (defect) densities (0.1%, 0.2%, and 0.4%). A total of 10,18 and 8 systems were stochastically analyzed for more than 200 energy values in the range $E \in [-1,1]$ in order to obtain the distributions shown in Figs. 3–5, respectively. A larger dispersion of the variance can be observed in doped

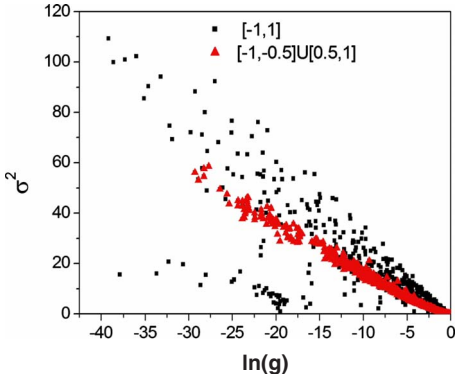

FIG. 4. (Color online) Conductance fluctuations σ^2 as a function of the average of the conductance natural logarithm $\langle \ln(g) \rangle$ for different N-doped $N_a=47$ AGNRs. Each point represents a statistical average over more than 500 equivalent replicas of the system. The systems differs for: scatter centers density (0.1%, 0.2% 0.4% cases), Fermi energy E, which belongs to the interval $[-1,1]$ and length $L=500,1000,1500,2000,3000,4000$. Red triangles evidence points for energies E in the intervals $[-1,-0.5]$ and $[0.5,1]$.

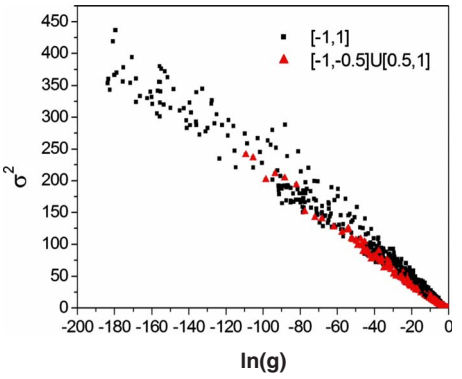

FIG. 5. (Color online) Conductance fluctuations σ^2 as a function of the average of the conductance natural logarithm $\langle \ln(g) \rangle$ for different V-damaged $N_a=47$ AGNRs. Each point represents a statistical average over more than 500 equivalent replica of the system. The systems differ for scatter centers density (0.2% 0.4% cases), Fermi energy E, which belongs to the interval $[-1,1]$, and length $L=500,1000,2000,4000$. Red triangles evidence values for energies E in the intervals $[-1,-0.5]$ and $[0.5,1]$.

AGNRs (Fig. 4) when compared to defected AGNRs (Fig. 5) and in semiconducting AGNRs (Fig. 3) when compared to semimetal AGNRs (Fig. 4). In order to qualitatively categorize these results, we note that small $\langle g \rangle$ small σ^2 points are related to energies near the conventional gap, while small $\langle g \rangle$ large σ^2 points are related to the spectral region where localization is caused by the interaction between electron and local scatter centers.

If the SPS was verified for all the energies in the interval considered (i.e., $E \in [-1,1]$ eV), we should expect that all the points (apart from the statistical errors) should collapse in a single line. Of course, in general, the results reported in Figs. 3–5 do not support the SPS hypothesis, and this finding seems in agreement with the similar results obtained in the framework of the Anderson model.[9] However, this kind of disorder realization is surely more realistic with respect to that simulated by the Anderson model and differences between the two different disordered realizations should be expected. Indeed, a careful analysis of results on the conductance fluctuations shows that the SPS hypothesis is verified in a rather large spectral region when disorder is due to defects or impurities at the concentration levels here investigated. This statement can be inferred looking at the red triangles in Figs. 3–5, which evidence $\sigma^2(E)$ for the same systems, for energies in the following ranges: $E \in [-1$ eV, -0.5 eV] and $E \in [0.5$ eV, 1 eV]. For these energy ranges, all the points clearly collapse in a single line irrespective to the dopant or impurity density or the energy values (please note that the number of points evidenced by triangles is exactly equal to the remaining ones). As a consequence, the SPS hypothesis seems to fail only near the charge neutrality point (or more exactly near the first plateau of the conductance of the corresponding pure system).

IV. FAILURE AND VALIDITY OF THE SINGLE SCALING PARAMETER HYPOTHESIS

The failure of the SPS hypothesis near $E=0$ can be explained according to density of states (DOS) based criteria

reported in the recent numerical and analytical studies for disordered systems, where disorder is realized in the framework of model Hamiltonians.[18–21] Indeed, according to the DOS criterion, the SPS is essentially controlled by another length scale $l_2(E)$ related to the DOS, which in the case of a single (isolated) band has the following expression:

$$l_2(E) = \sin[\pi N(E)/N_{\text{tot}}]^{-1}. \quad (3)$$

Here, the integrated DOS $N(E)$ and the total density N_{tot} are given by

$$N(E) = \int_{E_{bottom}}^{E} \text{DOS}(E)dE, \quad N_{tot} = \int_{E_{bottom}}^{E_{top}} \text{DOS}(E)dE, \quad (4)$$

and E_{bottom} and E_{top} are the band boundaries. The inequality $\xi(E) > l_2(\text{E})$ determines the region of the spectrum where the SPS should be valid. This criterion explains our results if the electron and hole bands of the GNRs are considered as two separate bands (i.e., $E_{bottom}=-\infty$, $E_{top}=0$ for the hole band, and $E_{bottom}=0$, $E_{top}=+\infty$ for the electron band). Here the criterion seems correct and SPS appears to be verified in spectral regions away from the first plateau of the conductance due to the concomitant strong increases of $\xi(E)$ and $N(E)$ [or the decrease of $l_2(E)$], i.e., the failure of SPS near the charge neutrality point is well categorized, as it was obtained for the Anderson model in a two dimensional square lattice when the energy belongs to the band tails.[20] In turn the results reported in Ref. 9 (obtained in GNRs where disorder is simulated again with the Anderson model) indicate a definitive failure of SPS in the whole energy spectrum that cannot be categorized by means of the DOS criterion. However, this relative discrepancy between the results in the framework of the Anderson model[9] and that here obtained with a realistic disorder realization can be also understood considering the strongly energy dependent localization features induced by the random scattering related to impurities and vacancies, while the random fluctuations of the on-site energy allow the realization of a disordered system which is in the strong localization regime for the whole energy spectrum.

Anyhow, the present and the previous numerical results on disordered systems demonstrate that quantitative valence of the DOS criterion is critical for a generic (i.e., not strictly one-dimensional, where its validity has been rigorously proven)[18] disordered system and it can simply be used for a qualitative analysis of the results.

V. DISCUSSION

This study evidences some experimentally verifiable features of the conductance distributions in devices based on doped or defected GNRs. The estimated quasigap, extending well away from the resonance levels, breaks the electron-hole symmetry. This finding is expected in a doped system while for the defected one it seems also more intriguing and merits particular dedicated experimental analysis. However, the experimental work should not be limited to the average conductance since conductance fluctuations also show important regularities when suitably analyzed. In particular, the conductance distribution should be "characteristic" of the particular GNR microstructural modification (black points in Figs. 3–5) when conductance measurements are performed in the low gate bias regime (SPS failure when E near the first plateau of the conductance) while it tends to be a universal function for quasi-Fermi energy E values away from this region (SPS validity red points in Figs. 3–5). In principle, conduction measurements could reproduce the condition here assumed: (a) equivalent systems with the same length can be investigated fixing the electrode distance (e.g., by means of nanoprobing techniques) and changing the measurement zone in the same long GNR, (b) the Fermi energy can be tuned using an additional (gate) electrode, (c) Raman measurements can be used to estimate the density of local scattering centers,[21,22] etc.

In view of the application to the quasigap control in GNRs, the vacancy inclusion (which has some natural vantages in terms of material processing since *V*s form by means of ion bombardments on graphene)[21] seems also more efficient than doping (compare Figs. 1 and 2) and very diluted controlled density can be sufficient to obtain a GNR device with the desired current levels in the ON and OFF states. However, the impact of the strong conductance fluctuations for energies in the quasigap regions to the device performance has to be critically addressed since they are not present, as we have noted (see again Fig. 3), in the conventional gap and could hinder the device functionality.

Finally, we would like to briefly comment the possible dependence of the current results on the calibration used. A different calibration, e.g., based on a different *ab initio* scheme or applied to a model extension, may of course lead to relative small quantitative changes in the outcomes of the numerical analysis. However, we do not expect any possible changes in the general aspects of the conductance features that were presented here in disordered GNRs due to the presence of local scattering centers.

[1] Y. W. Son, M. L. Cohen, and S. G. Louie, Phys. Rev. Lett. **97**, 216803 (2006).
[2] V. M. Pereira and A. H. Castro Neto, Phys. Rev. Lett. **103**, 046801 (2009).
[3] M. Y. Han, B. Ozyilman, Y. Zhang, and Ph. Kim, Phys. Rev. Lett. **98**, 206805 (2007).
[4] X. Li, X. Wang, L. Zhang, S. Lee, and H. Dai, Science **319**, 1229 (2008).
[5] B. Biel, X. Blase, F. Triozon, and S. Roche, Phys. Rev. Lett. **102**, 096803 (2009).
[6] B. Biel, X. Blase, F. Triozon, and S. Roche, Nano Lett. **9**, 2725 (2009).
[7] V. M. Pereira, J. M. B. Lopes dos Santos, and A. H. Castro Neto, Phys. Rev. B **77**, 115109 (2008).

[8] I. Deretzis and A. La Magna, Appl. Phys. Lett. **95**, 063111 (2009).
[9] A. La Magna, I. Deretzis, G. Forte, and R. Pucci, Phys. Rev. B **78**, 153405 (2008).
[10] A. La Magna, I Deretzis, G. Forte, and R. Pucci, Phys. Status Solidi B (to be published).
[11] C. Adessi, S. Roche, and X. Blasé, Phys. Rev. B **73**, 125414 (2006).
[12] I. Deretzis, G. Forte, A. Grassi, A. La Magna, G. Piccitto, and R. Pucci, arXiv:0905.3122 (unpublished).
[13] M. J. Frisch *et al.*, GAUSSIAN 03, Revision C.02. Gaussian, Inc., Wallingford, CT, 2004.
[14] T. C. Li and S. P. Lu, Phys. Rev. B **77**, 085408 (2008).
[15] J. J. Palacios, J. Fernández-Rossier, and L. Brey, Phys. Rev. B **77**, 195428 (2008).
[16] I. Deretzis and A. La Magna, Nanotechnology **17**, 5063 (2006).
[17] P. W. Anderson, D. J. Thouless, E. Abrahams, and D. S. Fisher, Phys. Rev. B **22**, 3519 (1980).
[18] L. I. Deych, A. A. Lisyansky, and B. L. Altshuler, Phys. Rev. Lett. **84**, 2678 (2000).
[19] L. I. Deych, M. V. Erementchouk, and A. A. Lisyansky, Phys. Rev. B **67**, 024205 (2003).
[20] A. M. Somoza, M. Ortuno, and J. Prior, Phys. Rev. Lett **99**, 116602 (2007).
[21] A. M. Somoza, J. Prior, and M. Ortuno, Phys. Rev. B **73**, 184201 (2006).
[22] G. Compagnini, F. Giannazzo, S. Sonde, V. Raineri, and E. Rimini, Carbon **47**, 3201 (2009).